Supporting Information

High Aspect Sub-Diffraction-Limit Photolithography via a Silver Superlens

Hong Liu,[†] Bing Wang,[†] Lin Ke,[†] Jie Deng,[†] Chan Choy Chum,[†] Lu Shen,[†] Stefan A. Maier,[*,‡] and Jinghua Teng[*,†]

[†] Institute of Materials Research and Engineering, Agency for Science, Technology and Research (A*STAR), 3 Research Link, Singapore 117602; [‡] Department of Physics, Imperial College London, London SW7 2AZ, UK.

[*,†] Email: jh-teng@imre.a-star.edu.sg, Tel: +65-6874-8590, Fax: +65-6872-0785;

[*,‡] Email: s.maier@imperial.ac.uk, Tel: +44-20-7594-6063, Fax: +44-20-7594-2077

RECEIVED DATE

1. Table S1. Key Features of Nano-gratings of Typical Superlens Lithography Experiments.

Ref. No. (Refer to Paper)	Illumination Wavelength (nm)	Mask Pattern	Half-Pitch of Mask Pattern (nm)	Depth of Photoresist Pattern (nm)
Ref. 21	365	Grating	60	~5-10
Ref. 27	365	Grating	85	< 5
Ref. 28	365	Grating	80	< 1
Ref. 29	380	Grating	30	< 6

2. Experimental Details

The fabrication of a superlens started from deposition of 40-nm chromium by electron beam evaporation (Denton Vacuum, Explorer) at room temperature onto an UV fused quartz wafer (UV grade, 15 mm x 15 mm x 0.4 mm) with a refractive index of 1.46. Photoresist of ZEP-520A mixed with anisole at a volumetric ratio of 1:1 was spin-coated on top of Cr film at 5000 rpm followed by a soft baking at 180°C for 2 minutes using a hotplate. Nano-patterning on the resist was done by electron beam lithography (ELS-7000, Elionix) at an exposure dose of 240 $\mu C/cm^2$, beam current of 50 pA and acceleration voltage of 100 kV followed by development in o-xylene for 30s. The sample was then subjected to an ion milling process (Nanoquest, Intlvac) under conditions of beam voltage/current of 300 V/110 mA, acceleration voltage/current of 100 V/6 mA, power of 180 W and vacuum of about 2.54×10^{-4} Torr for about 6 minutes. After that, the sample was soaked in Microposit remover 1165 (Shipley) for 12 hours followed by oxygen plasma etching (Oxford RIE) to remove the residual resist under a power of 100 W and O_2 flow of 80 sccm for 2 minutes. Multistep coatings of mr-I T85 (Micro Resist Technology, GmbH) were applied to planarize the Cr grating objects and serves as the spacer. The mr-I T85 (ε=2.415) is a transparent cyclic olefin copolymer (COC) and exhibits excellent transmission in UV region. Initially, the mr-I T85 was spin-coated at 3000 rpm to achieve a semi-conformal topographic surface. It was followed by a soft baking at 140°C for 2

minutes on a hotplate to create a hardened surface by evaporating the solvent as much as possible. It would prevent the mixing of the solvent with the next-coated mr-I T85 to facilitate the multistep spin coating. In this way, in total 6 layers had been coated to form a layer of about 600-nm thick, measured by variable angle spectroscopic ellipsometry (WVASE32, J. A. Woollam), to reduce the surface modulation. Its initial surface roughness (root-mean-square) was about 0.42 nm characterized by a multimode AFM (Veeco). This thick spacer deposited by multiple spin-coatings exhibited semi-conformal surface topography due to the embedded Cr objects. It had to be thinned as much as possible to avoid a significant decay of the evanescent field from objects. The thick spacer layer was etched down to about 20 nm using oxygen plasma etching (Sirus, Trion). The etching rate was measured to be about 0.7 nm/s at 20 W power, 20 sccm oxygen flow rate and 250 mTorr vacuum. Multi-cycle etching scheme was applied to precisely control the uniformity and the thickness. Each cycle took 30 s followed by an interval of 30 s to cool the chamber to stabilize the etch rate. The roughness was measured to be about 2.2 nm in-between the etching cycles. Once a desirable thickness was reached, a reflow process was applied at about 150°C on a hotplate for about 1 hour to smooth the spacer surface. The roughness was measured to be about 0.48 nm comparable to its initial surface. This reflow process has been identified very effective in reducing the surface roughness caused by the plasma etching process. Subsequently, a silver layer of 35-nm thick was deposited on top of the spacer through electron-beam evaporation (Explorer, Denton Vacuum) at a rate of about 3 nm/s. The roughness of Ag was measured to be ~1.6 nm. Negative tone photoresist of mr-UVL 6000 (Micro Resist Technology, GmbH) was spin-coated on Ag at 3000 rpm to produce a 100-nm thick imaging medium. The sample was then undergone I-line (365 nm in wavelength) flood-exposure using a mask aligner (MA8/MA6, Karl Suss) at an optimized dose of 480 mJ/cm^2 from the quartz substrate side followed by the developing in mr-Dev 600 (Micro Resist Technology, GmbH) for 50s and rinsed by IPA. Ultimately, the 2D and 3D sub-diffraction-limit optical images were transferred into the topographical profile of photoresist and characterized by AFM mapping. The control experiment on 2D nanostructures to verify the superlens lithography ability was performed by replacing the silver

layer with equally thick (35 nm) spacer of mr-I T85 and subjecting to the photolithography process under the same conditions.

An ultrahigh resolution Scanning Electron Microscope (ESM 9000, Elionix) was utilized to take the SEM pictures of the Cr objects. The surface topographies of the samples were characterized by a multimode AFM (Veeco) in tapping mode at a scan rate of about 0.5 Hz.

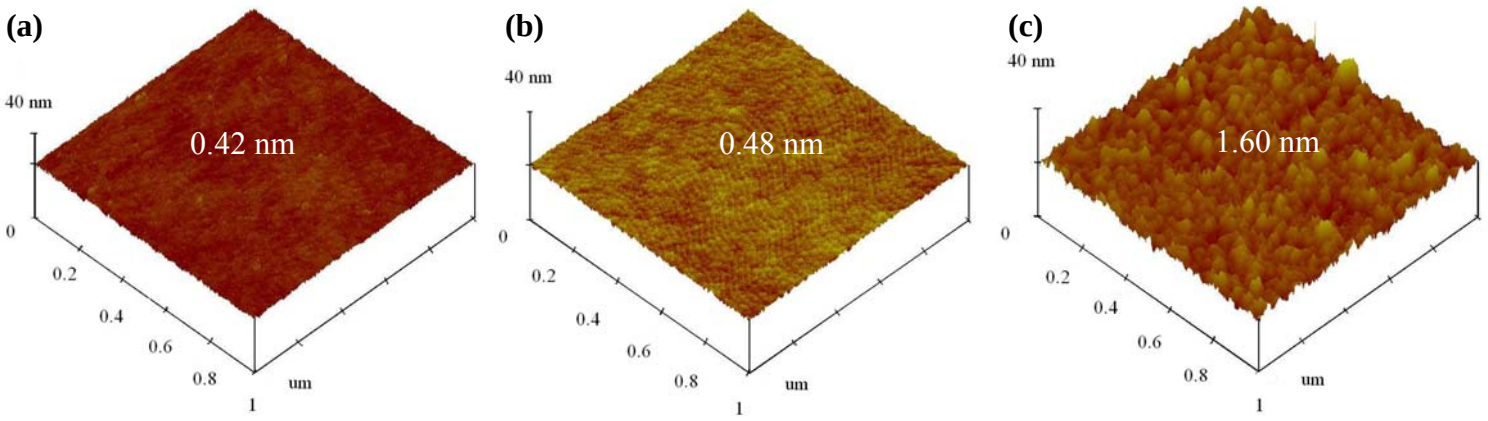

Figure S1. AFM images of polymer spacer and silver layer. The rms surface roughness measured for polymer spacer is (a) 0.42 nm (initial surface), (b) 0.48 nm (after reflow), and for Ag (c) 1.60 nm, respectively.

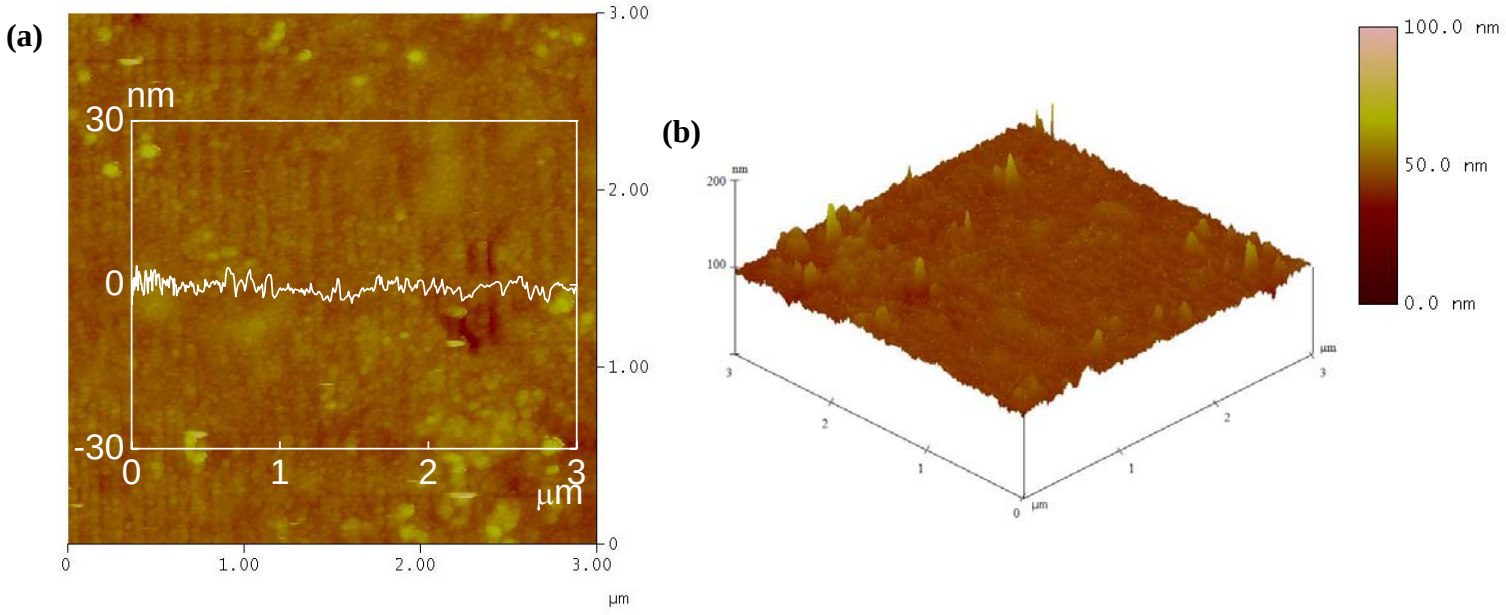

Figure S2. (a) AFM image (3 x 3 μm^2) of a control sample, in which the silver superlens has been replaced by a spacer of an equal thickness (35 nm). The cross section profile plotted in the inset shows a poor contrast of the developed pattern. (b) 3D plot of surface profile of the control sample depicts the sub-wavelength objects are irresolvable in the developed pattern. (The color scale for all AFM images is from 0 to 100 nm.)

3. Two-dimensional Point-Spread Function (PSF)

Figure S3 shows the schematic diagram of PSF computation. The metallic superlens possesses a refractive index of n_2 and a thickness of d. The refractive indices of the adjacent media of the metal are n_1 and n_3, respectively. The distance between the object and superlens is a and that between the image and the superlens is b.

The Green's function for the solution of the two-dimensional Helmhotz equation can be written as:

$$H(x,z) = \frac{j}{4} H_0^{(1)}(jk_1 |r|) \tag{1}$$

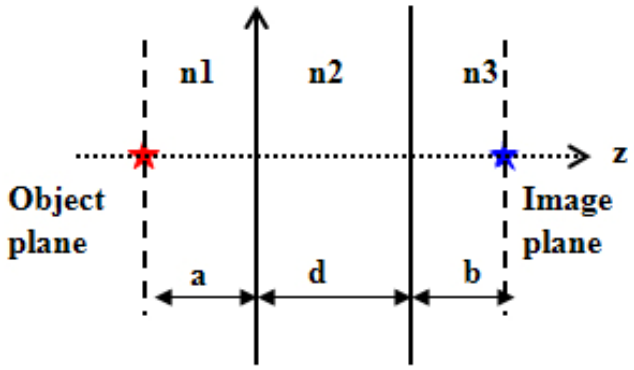

Figure S3. The scheme of PSF computation.

where $|r|=(x^2+z^2)^{1/2}$. The function could be used to represent the magnetic field of a point source as SPPs are TM polarized waves. The angular spectrum of the source is given as

$$\begin{aligned} \hat{H}(k_x,-a) &= \frac{1}{2\pi}\int_{-\infty}^{+\infty} H(x,0)\exp(-jk_x x)dx \\ &= \frac{j}{8\pi}\int_{-\infty}^{+\infty} H_0^{(1)}(jk_1|x|)\exp(-jk_x x)dx \end{aligned} \tag{2}$$

where $k_1=n_1k_0$. The field at $z=b+d$ can be represented as

$$H(x,b+d) = \int_{-\infty}^{+\infty} \hat{H}(k_x,b+d)\exp(jk_x x)dk_x \tag{3}$$

According to the *angular spectrum representation*, we have the PSF function

$$H(x,b+d)=\int_{-\infty}^{+\infty}\hat{H}(k_x,-a)OTF(k_x)\exp(jk_x x)dk_x \tag{4}$$

where OTF(k_x)=exp(j$k_{z1}a$)t(k_x)exp(jk_{z3}b) represents the *optical transfer function* (OTF) and can be calculated by RCWA method, $k_{z1}=(n_1^2k_1^2-k_x^2)^{1/2}$, $k_{z3}=(n_3^2k_3^2-k_x^2)^{1/2}$. The image of the object labeled by $O(x,-a)$ can be derived by convoluting the object with the PSF

$$I(x,b+d)=O(x,-a)*H(x,b+d)=\int_{-\infty}^{+\infty}O(\xi,-a)H(x-\xi,b+d)d\xi \tag{5}$$

4. Influence of Metal Surface Roughness

In our previous study[1], the surface roughness of metal is a key factor to affect the propagation of the surface plasmon polaritons (SPPs) on the metal film. The scattering of SPPs by the roughness has also been studied several years ago[2]. Based on this theory, we carry on an investigation on the influence of roughness on the PSF of the superlens. Basically, the strategy by making equivalence of the spatial roughness and the metal permittivity perturbation is quite straightforward. The roughness can be approximately described by a correlation function defined as

$$G(r)=R_q^2\exp(-\frac{r^2}{\sigma^2}) \tag{6}$$

where R_q, σ stand for the root-mean-square roughness and correlation length. The values of the two quantities can be extracted from the AFM data of the metal surface. According to the scatting theory analysis, the wave vector of SPPs undergoes a slight deviation $\Delta k_{SP}(\varepsilon_m,R_q,\sigma)$ due to the surface roughness. On the other hand, the wave vector deviation can also be activated by introducing a permittivity perturbation $\Delta\varepsilon_m$ of the metal. The two kinds of influence on the wave vector of SPPs are equivalent[3]. Thus we have $\Delta k_{SP}(\varepsilon_m,R_q,\sigma)= \Delta k_{SP}(\varepsilon_m+\Delta\varepsilon_m)$. By solving the equation, it is able to obtain the value of $\Delta\varepsilon_m$. By utilizing the effective metal permittivity $\varepsilon_m' =\varepsilon_m+\Delta\varepsilon_m$, the influence of the roughness can be taken account in the computation of the PSF.

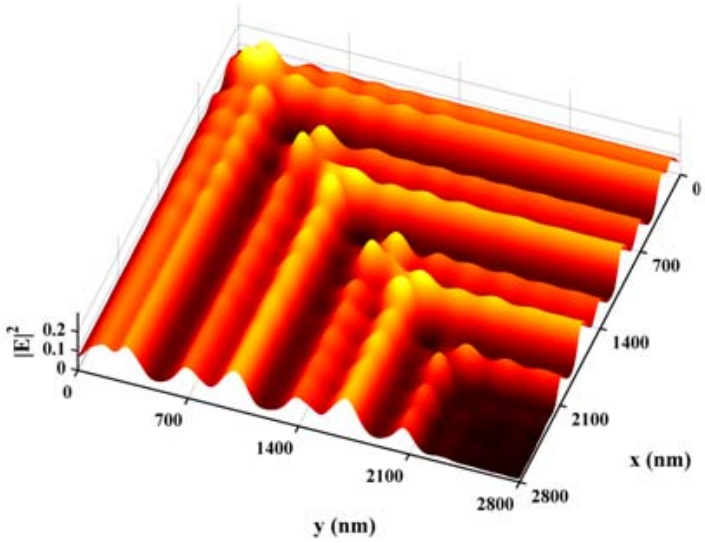

Figure S4. The 3D contour of electric field intensity distribution at a distance of 40 nm of control sample without an Ag superlens.

■ REFERENCES

(1) Liu, H. Wang, B.; Leong, E. S. P.; Yang, P.; Zong, Y.; Si. G.; Teng, J.; Maier, S. A. Enhanced surface plasmon resonance on a smooth silver film with a seed growth layer. *ACS Nano* **2010**, *4*, 3139-3146.

(2) Fontana, E.; Pantell, R. H. Characterization of multilayer rough surfaces by use of surface-plasmon spectroscopy. *Phys. Rev. B* **1988**, *37*, 3164-3182.

(3) Kolomenski, A.; Kolomenskii, A.; Noel, J.; Peng, S.; Schuessler, H. Propagation length of surface plasmons in a metal film with roughness. *Appl. Opt*. **2009**, *48*, 5683-5691.